

Gone But Not Forgotten: The HST Non-Detection of SN Ia 2011fe 11.5 yr After Explosion Further Restricts Single-Degenerate Progenitor Systems

M. A. TUCKER^{1, 2, 3, *} AND B. J. SHAPPEE⁴

¹Center for Cosmology and Astroparticle Physics, The Ohio State University, 191 West Woodruff Ave, Columbus, OH, USA

²Department of Astronomy, The Ohio State University, 140 West 18th Avenue, Columbus, OH, USA

³Department of Physics, The Ohio State University, 191 West Woodruff Ave, Columbus, OH, USA

⁴Institute for Astronomy, University of Hawaii, 2680 Woodlawn Drive, Honolulu HI 96822, USA

ABSTRACT

We present deep *Hubble Space Telescope* imaging of the nearby Type Ia supernova (SN Ia) 2011fe obtained 11.5 yr after explosion. No emission is detected at the SN location to a 1σ (3σ) limit of $F555W > 30.2$ (29.0) mag, or equivalently $M_V > 1.2$ (-0.1) mag, neglecting the distance uncertainty to M101. We constrain the presence of donor stars impacted by the SN ejecta with the strictest limits thus far on compact (i.e., $\log g \gtrsim 4$) companions. H-rich zero-age main-sequence companions with masses $\geq 2 M_\odot$ are excluded, a significant improvement upon the pre-explosion imaging limit of $\approx 5 M_\odot$. Main-sequence He stars with masses $\geq 0.5 M_\odot$ and subgiant He stars with masses $\lesssim 1 M_\odot$ are also disfavored by our late-time imaging. Synthesizing our limits on post-impact donors with previous constraints from pre-explosion imaging, early-time radio and X-ray observations, and nebular-phase spectroscopy, essentially all formation channels for SN 2011fe invoking a non-degenerate donor star at the time of explosion are unlikely.

Keywords: Type Ia supernovae (1728), Stellar mass loss (1613), Helium-rich stars (715), Interacting binary stars (801)

1. INTRODUCTION

The single-degenerate scenario for producing Type Ia supernovae (SNe Ia) invokes a non-degenerate donor star undergoing Roche Lobe overflow (RLOF) to transfer mass onto the white dwarf (WD) until reaching the necessary central densities for carbon ignition (Whelan & Iben 1973; Nomoto 1982). Mass transfer via RLOF restricts the distance between the WD and the donor to $a \lesssim 3R_*$ for semi-major axis a and companion radius R_* (Eggleton 1983) resulting in the SN Ia ejecta impacting the companion within moments of the explosion (e.g., Wheeler et al. 1975; Kasen 2010). The impact deposits energy into the envelope of the companion (e.g., Marietta et al. 2000; Boehner et al. 2017), heating and expanding the outer layers and becoming overluminous for $\sim 10^3$ yr (e.g., Podsiadlowski 2003; Shappee et al. 2013a).

tucker.957@osu.edu

* CCAPP Fellow

Searches for these post-impact donors have mostly been confined to nearby SN Ia remnants that are $\lesssim 1000$ yr old when the donor is still expected to be significantly overluminous. Some tentative candidates have been reported for Galactic and Magellanic Clouds SN Ia remnants (e.g., Ruiz-Lapuente et al. 2004; Ihara et al. 2007; Li et al. 2019) but no unambiguous surviving donor stars have been identified thus far (e.g., Schaefer & Pagnotta 2012; Kerzendorf et al. 2013; Pagnotta & Schaefer 2015; Kerzendorf et al. 2018; Shields et al. 2023; see Ruiz-Lapuente 2019 for a recent review). However, this experiment is observationally difficult due to the cost of obtaining deep spectroscopic follow-up for many targets and a limited number of nearby and young SN Ia remnants.

An alternative method for identifying post-impact companion stars is to obtain deep imaging for nearby SNe Ia many years after explosion once the SN has sufficiently faded. However, this is only possible for the most nearby ($\lesssim 10$ Mpc) SNe Ia due to crowding and faintness constraints. Do et al. (2021) recently searched for a post-impact donor star for SN 1972E but did not

Phase [d] ^a	10^{-2} counts/s	Vega mag.	M_V [mag]
1125	307 ± 7	24.47 ± 0.03	-4.56
1304	127 ± 4	25.45 ± 0.04	-3.58
1403	102 ± 2	25.71 ± 0.03	-3.32
1623	43.3 ± 5.3	26.63 ± 0.13	-2.40
1840	21.1 ± 3.5	27.43 ± 0.18	-1.60
2104	18.0 ± 3.1	27.57 ± 0.19	-1.46
2389	9.08 ± 2.93	28.34 ± 0.35	-0.69
4190	-0.29 ± 1.81	$> 28.96^b$	$> -0.07^b$

Table 1. *HST/WFC3 F555W photometry of SN 2011fe.*

^aRelative to t_{\max} ($\approx t_{\exp} + 18$). ^b 3σ limit.

find any candidates in *HST* imaging ≈ 33 yr after explosion. However, observations of SN 1972E near maximum light were obtained on photoelectric plates (e.g., Kirshner & Oke 1975) hindering rigorous comparison to modern explosion models.

In this Letter, we present deep *Hubble Space Telescope (HST)* imaging of the nearby and well-studied SN Ia 2011fe (Nugent et al. 2011) ≈ 11.5 yr after explosion to constrain the presence of post-impact companions. We adopt a distance to M101 of 6.4 ± 0.4 Mpc ($\mu = 29.03 \pm 0.14$ mag; Shappee & Stanek 2011) to ease comparisons with previous studies of SN 2011fe. We correct for the small amount of Milky Way reddening ($E(B-V)_{\text{MW}} = 0.008$ mag; Schlafly & Finkbeiner 2011) but do not correct for any host-galaxy reddening towards SN 2011fe as it is negligible (Patat et al. 2013). The date of explosion is MJD 55797 (Pereira et al. 2013).

2. HST OBSERVATIONS

We obtain deep imaging of SN 2011fe using the *HST* Wide Field Camera 3 (WFC3) UVIS module. Imaging was only conducted in the *F555W* filter due to the expected faintness of SN 2011fe at these epochs. Six images were obtained on UT 2023-03-04 (MJD 60007.55¹) corresponding to 4208 d (11.5 yr) after explosion with a total exposure time of 8400 s. To characterize the long-term evolution of SN 2011fe we include previous *HST* observations published by Shappee et al. (2017) and Tucker et al. (2022b) spanning $\approx 1100 - 2400$ d after explosion.

Individual images were aligned with TWEAKREG and combined with ASTRODRIZZLE (Avila et al. 2015) before performing point spread function (PSF) fitting photometry with DOLPHOT (Dolphin 2000, 2016). All images are analyzed simultaneously to ensure the location of SN 2011fe remains consistent across images. SN 2011fe

is formally undetected in the last epoch of *HST* imaging obtained 11.5 yr after the explosion so we validate the reported uncertainties by checking the photometry of nearby sources.

3. NON-DETECTION OF A POST-IMPACT COMPANION

We compare the *F555W* light curve of SN 2011fe to models of post-impact He (§3.1) and H-rich (§3.2) companions. The STSYNPHT software (STScI Development Team 2020) is used to impute synthetic *HST F555W* magnitudes (in the Vega system) using the T_{eff} and L_{\star} values taken from the models. When referring to the stellar properties of different models throughout the following sections, we always report the values at the moment of SN explosion (i.e., after mass transfer but before the ejecta impact) to avoid confusion.

3.1. He-star Donors

Models of the post-impact evolution for He-burning donors are taken from Pan et al. (2013, models HeWDad; see also Pan et al. 2010, 2012) and Liu et al. (2022, models He01r and He02r; see also Liu et al. 2013) which use the binary evolution results of Wang et al. (2009) to construct their initial binary systems. We also include the simulations of Liu et al. (2021) for a double-detonation explosion triggered by accretion from a low-mass MS He-star (models A, B, and C).

Fig. 3 shows that most He-star models are incompatible with the observed *F555W* light curve of SN 2011fe. The two lowest-mass He donors ($0.30 M_{\odot}$ and $0.40 M_{\odot}$) from Liu et al. (2021) would not be detected but the $0.50 M_{\odot}$ model would have produced a $\approx 2\sigma$ detection. Thus, we disfavor MS He-burning donors with masses $\gtrsim 0.50 M_{\odot}$ because the thermal timescale decreases with increasing mass. The inverse is true for the SG models, where more massive donors produce more extended envelopes and thus increase the thermalization timescale. The $1.0 M_{\odot}$ model from Liu et al. (2022) would have been detected at $\approx 2\sigma$ in our *HST* observations so we disfavor $\lesssim 1 M_{\odot}$ SG He-stars.

3.2. H-rich Donors

Unlike He-stars, most H-burning MS donors remain undetectable ($F555W \gtrsim 32$ mag) over the observational baseline (Pan et al. 2012; Rau & Pan 2022). This is attributed to H-rich stars having larger radii at a given mass compared to He stars and thus respond slower and reach lower maximum luminosities (e.g., Pan et al. 2012, 2013). However, there are a few cases where H-rich donors can be assessed with the *HST* non-detection.

Rau & Pan (2022) compute models for zero-age main-sequence (ZAMS) companions assuming RLOF and ex-

¹ Weighted by the exposure time for each observation.

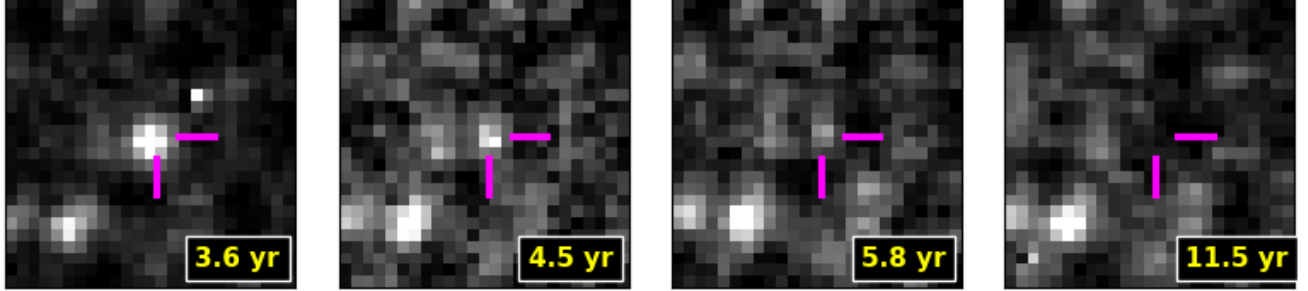


Figure 1. Image cutouts centered on SN 2011fe for several *HST* epochs. The time between explosion and observation is denoted in the lower-right corner of each panel.

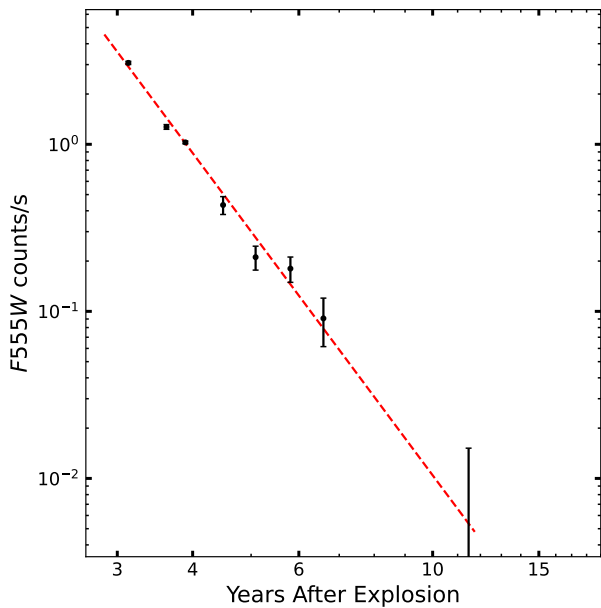


Figure 2. $F555W$ light curve of SN 2011fe provided in Table 1. The red dashed line shows a simple power-law fit with $f \propto t^{-5}$ highlighting the steadily declining flux. The last observation is not included when fitting the power-law model.

tend the simulations to binary systems with companions beyond the canonical RLOF separation. While such systems are somewhat contrived due to fine-tuning the mass transfer and time of ignition for the C/O WD, the larger separations produce shallower energy deposition which, in turn, corresponds to increased post-impact luminosities and shorter thermalization timescales (e.g., Fig. 8 in Rau & Pan 2022).

Fig. 4 shows that the $2 M_{\odot}$ donor from Rau & Pan (2022) is disfavored for all binary separations. The $1.5 M_{\odot}$ model would have been likely detected ($\approx 2\sigma$) at $a \gtrsim 3R_{\star}$ but only marginally detected if the system was in RLOF. The two lower-mass models from Rau & Pan (2022), $0.8 M_{\odot}$ and $1 M_{\odot}$, are not constrained by

our observations regardless of separation due to their low peak luminosities ($\lesssim 10 L_{\odot}$).

The MS models computed by Pan et al. (2012) with masses of $\approx 1.2 - 1.9 M_{\odot}$ remain undetectable for another century or more. The differences between these models and the similar-mass models computed by Rau & Pan (2022) are attributed to the density structure of the donor star at the time of impact. Pan et al. (2012) model the full binary evolution, including mass transfer, when constructing their donor stars whereas Rau & Pan (2022) assume ZAMS stars to facilitate parameter exploration and dependencies on SN properties. These differences will be discussed further below.

4. DISCUSSION

The compressibility of the stellar envelope determines the thermal response timescale (Pan et al. 2012). Stars with high surface gravities confine the energy deposition to the outermost layers whereas the energy is deposited deeper into the stellar interior for low $\log g$ donors (cf. Fig. 5 from Rau & Pan 2022). This work constrains a complimentary parameter space to other searches for non-degenerate donor stars in SN 2011fe as we are most sensitive to high $\log g$ companions.

All but the lowest-mass MS He donors are excluded by our late-time imaging of SN 2011fe. The $0.5 M_{\odot}$ model from Liu et al. (2021) would be detected at $\approx 2\sigma$ so $\gtrsim 0.5 M_{\odot}$ MS He donors are disfavored. For an assumed accreted He mass of $\approx 0.05 M_{\odot}$ and an accretion efficiency of 50%², our results restrict MS He donors to $\lesssim 0.6 M_{\odot}$ at the onset of RLOF. While such systems are observed in the Milky Way (i.e., AM CVn binaries) they are likely the progenitors of faint and spectroscopically

² The adopted 50% accretion efficiency is purely instructive as the true accretion efficiency depends sensitively on the mass transfer rate (e.g., Piersanti et al. 2014; Wu et al. 2017). He shells with masses $\gtrsim 0.05 M_{\odot}$ produce distinct early-time signatures (e.g., Polin et al. 2019; Collins et al. 2022) that are not observed in SN 2011fe.

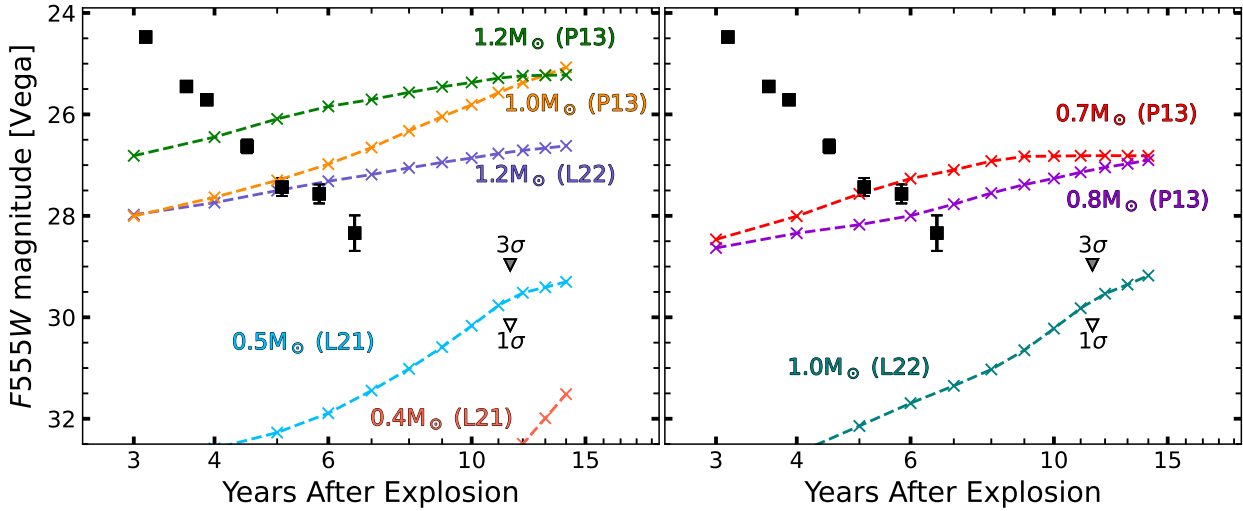


Figure 3. Comparison between the light curve of SN 2011fe (black squares) with models of post-impact He-star companions (colored lines). The inverted triangles show the 1σ (open triangle) and 3σ (filled triangle) non-detection limits. The uncertainty in the distance modulus is ≈ 0.14 mag. *Left:* Main-sequence He-star companions from Pan et al. (2013, P13), Liu et al. (2021, L21), and Liu et al. (2022, L22). *Right:* Similar to the left panel except for subgiant He-star companions.

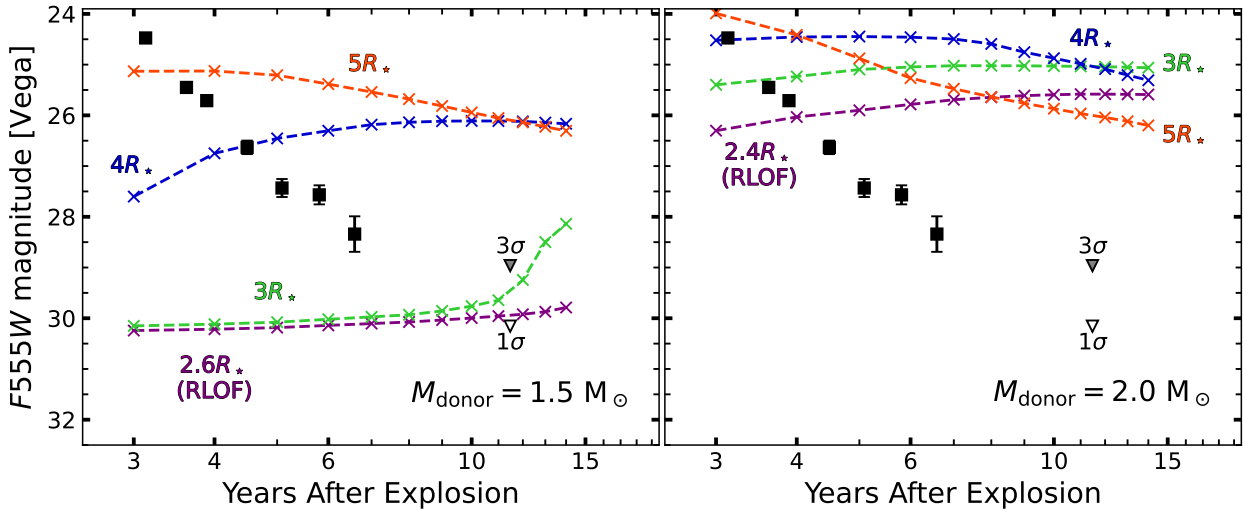


Figure 4. Comparison between the light curve of SN 2011fe (black squares) with the post-impact H-rich MS companions of Rau & Pan (2022) with masses of $M_{\text{donor}} = 1.5 M_{\odot}$ (left) and $M_{\text{donor}} = 2 M_{\odot}$ (right) for different binary separations. The uncertainty in the distance is ≈ 0.14 mag.

peculiar SNe Ia (e.g., Bildsten et al. 2007; Neunteufel et al. 2019) instead of normal SNe Ia such as SN 2011fe.

The SG He donors follow an opposing trend, with more massive companions being harder to detect due to the increasing mass of the envelope which increases the heating depth and thermalization timescale. SG He donors with masses $\gtrsim 1.1 M_{\odot}$ (again assuming the mass of the He shell is $\lesssim 0.05 M_{\odot}$ and an accretion efficiency of 50%) are disfavored by our late-time imaging. Higher-mass SG He donors are inconsistent with pre-explosion

imaging (Li et al. 2011; Graur et al. 2014) so binaries with SG He stars are disfavored for SN 2011fe.

H-rich donors are less constrained by our latest epoch of *HST* imaging but complement existing non-detections of H-rich companions. All ZAMS H-rich donors with masses $\gtrsim 2 M_{\odot}$ are disfavored, representing a distinct improvement on the pre-explosion limit of $\approx 5 M_{\odot}$ (Li et al. 2011). $1.5 M_{\odot}$ donors beyond the RLOF radius are also disfavored, but a $1.5 M_{\odot}$ donor undergoing RLOF would be only marginally detected and $\leq 1 M_{\odot}$ donors

at $< 5 R_\star$ are unconstrained by the late-time *HST* imaging due to their low post-impact luminosity ($\lesssim 10 L_\odot$).

However, these same H-rich ZAMS donors are already disfavored along separate lines of evidence. The impacting ejecta will strip or ablate material off the surface of the donor and heating from the radioactively-decaying ejecta will produce strong H emission lines in the nebular phase (Mattila et al. 2005; Botyánszki et al. 2018; Dessart et al. 2020). H emission is not seen in the spectra of SN 2011fe (Shappee et al. 2013b) out to 1000 d after explosion (Graham et al. 2015; Taubenberger et al. 2015) and the formal limits on unbound donor material are $\lesssim 10^{-3} M_\odot$ (e.g., Fig. 6 in Tucker et al. 2022a). All post-impact ZAMS donors not excluded by our *HST* observations produce $\gtrsim 0.05 M_\odot$ of unbound material, inconsistent with nebular-phase observations (Shappee et al. 2013b; Lundqvist et al. 2015). Thus, H-rich donors are also disfavored for SN 2011fe.

One potential caveat for future observational and theoretical work on post-impact donor stars is the effect of the donor star structure. We qualitatively compare the H-rich $2 M_\odot$ ZAMS model at RLOF from Rau & Pan (2022) to Model B from Pan et al. (2012) with a mass of $1.92 M_\odot$ at the time of the explosion. While the right panel of Fig. 4 shows the former is disfavored by our observations, the latter is unconstrained by our observations ($F555W > 32$ mag). The difference between these models is the density profile of the companion at the moment of impact, as the models of Pan et al. (2012) include mass transfer prior to explosion instead of adopting a ZAMS density profile. The mass transfer reduces the envelope density compared to a ZAMS star with identical mass. This is supported by the higher amount of unbound mass in the Pan et al. (2012) evolved model ($\approx 15\%$) compared to the Rau & Pan (2022) ZAMS model ($\approx 10\%$). This qualitative comparison highlights the differences in post-impact evolution with and without including the effects of mass loss on the donor star structure.

The ≈ 1 mag difference between the $1.2 M_\odot$ MS He-star models of Pan et al. (2013) and Liu et al. (2022) seen in Fig. 3 further highlights the effect of mass-transfer on the donor structure. Despite the donors having similar mass at the moment the WD explodes, they began with different masses³ and experienced different mass-transfer histories. The observed difference in synthetic $F555W$ (and the underlying L_\star estimates) are driven by

inherent differences in the donor’s internal density profile. We encourage future simulation efforts to explore the dependence on different density profiles produced by realistic mass-transfer histories.

SN 2011fe has been a boon for understanding the complex physics governing SN Ia explosions. These observations, at an unprecedented 11.5 yr after explosion, provide the strongest limits on He-rich donors in addition to further disfavoring H-rich donors. Assessing our new imaging in conjunction with prior limits on the progenitor system of SN 2011fe (Li et al. 2011; Nugent et al. 2011; Bloom et al. 2012; Margutti et al. 2012; Chomiuk et al. 2012; Brown et al. 2012), almost all non-degenerate donor stars are observationally disfavored. The remaining scenarios that cannot be formally excluded, such as very low-mass ($\lesssim 0.6 M_\odot$) He donors, are disfavored by rate arguments given that SN 2011fe is a quintessential example of the SN Ia population.

Facility: HST (WFC3/UVIS)

Software: astropy (Astropy Collaboration et al. 2022), numpy (Harris et al. 2020), matplotlib (Hunter 2007), pandas (Reback et al. 2022), scipy (Virtanen et al. 2020), lmfit (Newville et al. 2014), synphot (STScI Development Team 2018)

ACKNOWLEDGEMENTS

We thank Michelle Tucker and Jen van Saders for useful discussions.

³ The initial He-donor masses for the $\approx 1.2 M_\odot$ models of Pan et al. (2013) and Liu et al. (2022) are $1.8 M_\odot$ and $1.55 M_\odot$, respectively, at the onset of RLOF.

REFERENCES

- Astropy Collaboration, Price-Whelan, A. M., Lim, P. L., et al. 2022, ApJ, 935, 167, doi: [10.3847/1538-4357/ac7c74](https://doi.org/10.3847/1538-4357/ac7c74)
- Avila, R. J., Hack, W., Cara, M., et al. 2015, in Astronomical Society of the Pacific Conference Series, Vol. 495, Astronomical Data Analysis Software and Systems XXIV (ADASS XXIV), ed. A. R. Taylor & E. Rosolowsky, 281, doi: [10.48550/arXiv.1411.5605](https://doi.org/10.48550/arXiv.1411.5605)
- Bildsten, L., Shen, K. J., Weinberg, N. N., & Nelemans, G. 2007, ApJL, 662, L95, doi: [10.1086/519489](https://doi.org/10.1086/519489)
- Bloom, J. S., Kasen, D., Shen, K. J., et al. 2012, ApJL, 744, L17, doi: [10.1088/2041-8205/744/2/L17](https://doi.org/10.1088/2041-8205/744/2/L17)
- Boehner, P., Plewa, T., & Langer, N. 2017, MNRAS, 465, 2060, doi: [10.1093/mnras/stw2737](https://doi.org/10.1093/mnras/stw2737)
- Botyánszki, J., Kasen, D., & Plewa, T. 2018, ApJL, 852, L6, doi: [10.3847/2041-8213/aaa07b](https://doi.org/10.3847/2041-8213/aaa07b)
- Brown, P. J., Dawson, K. S., de Pasquale, M., et al. 2012, ApJ, 753, 22, doi: [10.1088/0004-637X/753/1/22](https://doi.org/10.1088/0004-637X/753/1/22)
- Chomiuk, L., Soderberg, A. M., Moe, M., et al. 2012, ApJ, 750, 164, doi: [10.1088/0004-637X/750/2/164](https://doi.org/10.1088/0004-637X/750/2/164)
- Collins, C. E., Gronow, S., Sim, S. A., & Röpke, F. K. 2022, MNRAS, 517, 5289, doi: [10.1093/mnras/stac2665](https://doi.org/10.1093/mnras/stac2665)
- Dessart, L., Leonard, D. C., & Prieto, J. L. 2020, A&A, 638, A80, doi: [10.1051/0004-6361/202037854](https://doi.org/10.1051/0004-6361/202037854)
- Do, A., Shappee, B. J., De Cuyper, J.-P., et al. 2021, MNRAS, 508, 3649, doi: [10.1093/mnras/stab2660](https://doi.org/10.1093/mnras/stab2660)
- Dolphin, A. 2016, DOLPHOT: Stellar photometry, Astrophysics Source Code Library, record ascl:1608.013. <http://ascl.net/1608.013>
- Dolphin, A. E. 2000, PASP, 112, 1383, doi: [10.1086/316630](https://doi.org/10.1086/316630)
- Eggleton, P. P. 1983, ApJ, 268, 368, doi: [10.1086/160960](https://doi.org/10.1086/160960)
- Graham, M. L., Nugent, P. E., Sullivan, M., et al. 2015, MNRAS, 454, 1948, doi: [10.1093/mnras/stv1888](https://doi.org/10.1093/mnras/stv1888)
- Graur, O., Maoz, D., & Shara, M. M. 2014, MNRAS, 442, L28, doi: [10.1093/mnrasl/slu052](https://doi.org/10.1093/mnrasl/slu052)
- Harris, C. R., Millman, K. J., van der Walt, S. J., et al. 2020, Nature, 585, 357, doi: [10.1038/s41586-020-2649-2](https://doi.org/10.1038/s41586-020-2649-2)
- Hunter, J. D. 2007, Computing in Science and Engineering, 9, 90, doi: [10.1109/MCSE.2007.55](https://doi.org/10.1109/MCSE.2007.55)
- Ihara, Y., Ozaki, J., Doi, M., et al. 2007, PASJ, 59, 811, doi: [10.1093/pasj/59.4.811](https://doi.org/10.1093/pasj/59.4.811)
- Kasen, D. 2010, ApJ, 708, 1025, doi: [10.1088/0004-637X/708/2/1025](https://doi.org/10.1088/0004-637X/708/2/1025)
- Kerzendorf, W. E., Strampelli, G., Shen, K. J., et al. 2018, MNRAS, 479, 192, doi: [10.1093/mnras/sty1357](https://doi.org/10.1093/mnras/sty1357)
- Kerzendorf, W. E., Yong, D., Schmidt, B. P., et al. 2013, ApJ, 774, 99, doi: [10.1088/0004-637X/774/2/99](https://doi.org/10.1088/0004-637X/774/2/99)
- Kirshner, R. P., & Oke, J. B. 1975, ApJ, 200, 574, doi: [10.1086/153824](https://doi.org/10.1086/153824)
- Li, C.-J., Kerzendorf, W. E., Chu, Y.-H., et al. 2019, ApJ, 886, 99, doi: [10.3847/1538-4357/ab4a03](https://doi.org/10.3847/1538-4357/ab4a03)
- Li, W., Bloom, J. S., Podsiadlowski, P., et al. 2011, Nature, 480, 348, doi: [10.1038/nature10646](https://doi.org/10.1038/nature10646)
- Liu, Z.-W., Röpke, F. K., & Zeng, Y. 2022, ApJ, 928, 146, doi: [10.3847/1538-4357/ac5517](https://doi.org/10.3847/1538-4357/ac5517)
- Liu, Z.-W., Röpke, F. K., Zeng, Y., & Heger, A. 2021, A&A, 654, A103, doi: [10.1051/0004-6361/202141518](https://doi.org/10.1051/0004-6361/202141518)
- Liu, Z.-W., Pakmor, R., Seitenzahl, I. R., et al. 2013, ApJ, 774, 37, doi: [10.1088/0004-637X/774/1/37](https://doi.org/10.1088/0004-637X/774/1/37)
- Lundqvist, P., Nyholm, A., Taddia, F., et al. 2015, A&A, 577, A39, doi: [10.1051/0004-6361/201525719](https://doi.org/10.1051/0004-6361/201525719)
- Margutti, R., Soderberg, A. M., Chomiuk, L., et al. 2012, ApJ, 751, 134, doi: [10.1088/0004-637X/751/2/134](https://doi.org/10.1088/0004-637X/751/2/134)
- Marietta, E., Burrows, A., & Fryxell, B. 2000, ApJS, 128, 615, doi: [10.1086/313392](https://doi.org/10.1086/313392)
- Mattila, S., Lundqvist, P., Sollerman, J., et al. 2005, A&A, 443, 649, doi: [10.1051/0004-6361:20052731](https://doi.org/10.1051/0004-6361:20052731)
- Neunteufel, P., Yoon, S. C., & Langer, N. 2019, A&A, 627, A14, doi: [10.1051/0004-6361/201935322](https://doi.org/10.1051/0004-6361/201935322)
- Newville, M., Stensitzki, T., Allen, D. B., & Ingargiola, A. 2014, LMFIT: Non-Linear Least-Square Minimization and Curve-Fitting for Python, 0.8.0, Zenodo, Zenodo, doi: [10.5281/zenodo.11813](https://doi.org/10.5281/zenodo.11813)
- Nomoto, K. 1982, ApJ, 253, 798, doi: [10.1086/159682](https://doi.org/10.1086/159682)
- Nugent, P. E., Sullivan, M., Cenko, S. B., et al. 2011, Nature, 480, 344, doi: [10.1038/nature10644](https://doi.org/10.1038/nature10644)
- Pagnotta, A., & Schaefer, B. E. 2015, ApJ, 799, 101, doi: [10.1088/0004-637X/799/1/101](https://doi.org/10.1088/0004-637X/799/1/101)
- Pan, K.-C., Ricker, P. M., & Taam, R. E. 2010, ApJ, 715, 78, doi: [10.1088/0004-637X/715/1/78](https://doi.org/10.1088/0004-637X/715/1/78)
- . 2012, ApJ, 760, 21, doi: [10.1088/0004-637X/760/1/21](https://doi.org/10.1088/0004-637X/760/1/21)
- . 2013, ApJ, 773, 49, doi: [10.1088/0004-637X/773/1/49](https://doi.org/10.1088/0004-637X/773/1/49)
- Patat, F., Cordiner, M. A., Cox, N. L. J., et al. 2013, A&A, 549, A62, doi: [10.1051/0004-6361/201118556](https://doi.org/10.1051/0004-6361/201118556)
- Pereira, R., Thomas, R. C., Aldering, G., et al. 2013, A&A, 554, A27, doi: [10.1051/0004-6361/201221008](https://doi.org/10.1051/0004-6361/201221008)
- Piersanti, L., Tornambé, A., & Yungelson, L. R. 2014, MNRAS, 445, 3239, doi: [10.1093/mnras/stu1885](https://doi.org/10.1093/mnras/stu1885)
- Podsiadlowski, P. 2003, arXiv e-prints, astro, doi: [10.48550/arXiv.astro-ph/0303660](https://doi.org/10.48550/arXiv.astro-ph/0303660)
- Polin, A., Nugent, P., & Kasen, D. 2019, ApJ, 873, 84, doi: [10.3847/1538-4357/aafb6a](https://doi.org/10.3847/1538-4357/aafb6a)
- Rau, S.-J., & Pan, K.-C. 2022, ApJ, 933, 38, doi: [10.3847/1538-4357/ac7153](https://doi.org/10.3847/1538-4357/ac7153)
- Reback, J., jbrockmendel, McKinney, W., et al. 2022, pandas-dev/pandas: Pandas 1.4.2, v1.4.2, Zenodo, Zenodo, doi: [10.5281/zenodo.3509134](https://doi.org/10.5281/zenodo.3509134)

- Ruiz-Lapuente, P. 2019, NewAR, 85, 101523, doi: [10.1016/j.newar.2019.101523](https://doi.org/10.1016/j.newar.2019.101523)
- Ruiz-Lapuente, P., Comeron, F., Méndez, J., et al. 2004, Nature, 431, 1069, doi: [10.1038/nature03006](https://doi.org/10.1038/nature03006)
- Schaefer, B. E., & Pagnotta, A. 2012, Nature, 481, 164, doi: [10.1038/nature10692](https://doi.org/10.1038/nature10692)
- Schlafly, E. F., & Finkbeiner, D. P. 2011, ApJ, 737, 103, doi: [10.1088/0004-637X/737/2/103](https://doi.org/10.1088/0004-637X/737/2/103)
- Shappee, B. J., Kochanek, C. S., & Stanek, K. Z. 2013a, ApJ, 765, 150, doi: [10.1088/0004-637X/765/2/150](https://doi.org/10.1088/0004-637X/765/2/150)
- Shappee, B. J., & Stanek, K. Z. 2011, ApJ, 733, 124, doi: [10.1088/0004-637X/733/2/124](https://doi.org/10.1088/0004-637X/733/2/124)
- Shappee, B. J., Stanek, K. Z., Kochanek, C. S., & Garnavich, P. M. 2017, ApJ, 841, 48, doi: [10.3847/1538-4357/aa6eab](https://doi.org/10.3847/1538-4357/aa6eab)
- Shappee, B. J., Stanek, K. Z., Pogge, R. W., & Garnavich, P. M. 2013b, ApJL, 762, L5, doi: [10.1088/2041-8205/762/1/L5](https://doi.org/10.1088/2041-8205/762/1/L5)
- Shields, J. V., Arunachalam, P., Kerzendorf, W., et al. 2023, ApJL, 950, L10, doi: [10.3847/2041-8213/acd6a0](https://doi.org/10.3847/2041-8213/acd6a0)
- STScI Development Team. 2018, synphot: Synthetic photometry using Astropy, Astrophysics Source Code Library, record ascl:1811.001. <http://ascl.net/1811.001>
- . 2020, stsynphot: synphot for HST and JWST, Astrophysics Source Code Library, record ascl:2010.003. <http://ascl.net/2010.003>
- Taubenberger, S., Elias-Rosa, N., Kerzendorf, W. E., et al. 2015, MNRAS, 448, L48, doi: [10.1093/mnrasl/slu201](https://doi.org/10.1093/mnrasl/slu201)
- Tucker, M. A., Ashall, C., Shappee, B. J., et al. 2022a, ApJL, 926, L25, doi: [10.3847/2041-8213/ac4fb0](https://doi.org/10.3847/2041-8213/ac4fb0)
- Tucker, M. A., Shappee, B. J., Kochanek, C. S., et al. 2022b, MNRAS, 517, 4119, doi: [10.1093/mnras/stac2873](https://doi.org/10.1093/mnras/stac2873)
- Virtanen, P., Gommers, R., Oliphant, T. E., et al. 2020, Nature Methods, 17, 261, doi: [10.1038/s41592-019-0686-2](https://doi.org/10.1038/s41592-019-0686-2)
- Wang, B., Meng, X., Chen, X., & Han, Z. 2009, MNRAS, 395, 847, doi: [10.1111/j.1365-2966.2009.14545.x](https://doi.org/10.1111/j.1365-2966.2009.14545.x)
- Wheeler, J. C., Lecar, M., & McKee, C. F. 1975, ApJ, 200, 145, doi: [10.1086/153771](https://doi.org/10.1086/153771)
- Whelan, J., & Iben, Icko, J. 1973, ApJ, 186, 1007, doi: [10.1086/152565](https://doi.org/10.1086/152565)
- Wu, C., Wang, B., Liu, D., & Han, Z. 2017, A&A, 604, A31, doi: [10.1051/0004-6361/201630099](https://doi.org/10.1051/0004-6361/201630099)